FSH-dependent enzyme that converts androgen to estrogen in the granulosa cell (*10*). The selective binding of FSH to granulosa cells not only generates FSH receptors and aromatase activity but also induces LH receptors (*11*). Thus, FSH deficiency during the follicular phase may result in lowered numbers of LH receptors for the luteal phase, and thereby diminish the luteotropic activity of LH on luteal cells. This interpretation is consistent with the observation that in women with a short luteal phase, treatment with human chorionic gonadotropin (hCG) frequently fails to rescue luteal function (*12*). In addition, a decreased hCG sensitivity of luteal cells in vitro has been observed in monkeys with follicular phase FSH deficiency induced by porcine follicular fluid (*12*).

Although LRF agonists are also effective luteolytic agents, the presence of a narrow window of maximum sensitivity during the luteal phase of the cycle detracts from the practical application of those agonists as contraceptives (*13*). Luteolysis does not occur with the mode of administration used in our studies; fertility is probably curtailed because of the early regression of the corpus luteum which occurs 1 to 2 days before the expected date of nidation (days 8 to 9 after the LH surge) (*14*), and the resulting inadequate development of the estrogen-progestin–dependent endometrium. The convenience of timing administration of the LRF agonist at the onset of menstruation represents a major advantage for practical application to fertility control and offers the possibility for providing a "once a month pill."

K. L. SHEEHAN
R. F. CASPER
S. S. C. YEN*

Department of Reproductive Medicine (T-002), School of Medicine, and
General Clinical Research Center, University of California, San Diego, La Jolla 92093

References and Notes

1. G. S. Jones and V. Madrigal-Castro, *Fertil. Steril.* **21**, 1 (1970); B. M. Sherman and S. G. Korenman, *J. Clin. Endocrinol. Metab.* **38**, 89 (1974); *ibid.* **39**, 145 (1974); T. Annus, I. E. Thompson, M. L. Taymor, *Obstet. Gynecol.* **55**, 705 (1980).
2. J. W. Wilks, G. D. Hodgen, G. T. Ross, *J. Clin. Endocrinol. Metab.* **43**, 1261 (1976); T. E. Nass, D. J. Dierschke, J. R. Clarke, P. A. Meller, K. K. Schillo, *Ovarian Follicular and Corpus Luteum Function*, C. P. Channing, J. Marsh, W. Sadler, Eds. (Plenum, New York, 1979), p. 519; G. S. de Zerega and G. D. Hodgen, *Fertil. Steril.* **35**, 489 (1981).
3. J. L. H. Horta, J. G. Fernandez, L. B. De Soto, V. Cortex-Gallegos, *Obstet. Gynecol.* **49**, 705 (1977); G. S. di Zerega and G. D. Hodgen, *Endocrinol. Rev.* **2**, 27 (1981).
4. D. R. Tredway, D. R. Mishell, D. L. Moyer, *Am. J. Obstet. Gynecol.* **117**, 1031 (1973); D. L. Rosenfeld and C. R. Garcia, *Fertil. Steril.* **27**, 1256 (1976); A. C. Wentz, *ibid.* **33**, 121 (1980).
5. C. Bergquist, S. J. Nillius, L. Wide, *J. Clin. Endocrinol. Metab.* **49**, 472 (1979); D. Rabin and L. W. McNeil, *ibid.* **51**, 873 (1980); D. Heber and R. S. Swerdloff, *ibid.* **52**, 171 (1981); R. F. Casper and S. S. C. Yen, *ibid.* **53**, 1056 (1981).
6. S. S. C. Yen, O. Llerena, B. Little, O. H. Pearson, *J. Clin. Endocrinol. Metab.* **28**, 1763 (1968); S. S. C. Yen, L. A. Llerena, O. H. Pearson, A. S. Little, *ibid.* **30**, 325 (1970); D. C. Anderson, B. R. Hopper, B. L. Lasley, S. S. C. Yen, *Steroids* **28**, 179 (1976); G. W. DeVane, N. M. Czekala, H. L. Judd, S. S. C. Yen, *Am. J. Obstet. Gynecol.* **121**, 495 (1975).
7. The [D-Trp^6,Pro^{9}NEt]LRF used in this study was synthesized and generously provided by W. Vale and J. Rivier of the Salk Institute, La Jolla, Calif. Use of the 50-μg dose of LRF agonist was based on our previous dose-response study in the follicular phase of the menstrual cycle [R. F. Casper, K. L. Sheehan, S. S. C. Yen, *J. Clin. Endocrinol. Metab.* **50**, 179 (1979)], in which a maximum gonadotropin response and significant LH elevation lasting for at least 24 hours were achieved after a single 50-μg dose.
8. S. S. C. Yen, G. L. Lasley, C. F. Wang, H. Leblanc, T. M. Siler, *Recent Prog. Horm. Res.* **31**, 321 (1975).
9. R. F. Casper, G. F. Erickson, R. W. Rebar, S. S. C. Yen, *Fertil. Steril.*, in press; R. H. Asch, M. V. Sickle, J. P. Balmaceda, C. A. Eddy, D. H. Coy, A. V. Schally, *J. Clin. Endocrinol. Metab.* **53**, 215 (1981).
10. K. J. Ryan, A. Petro, J. Kaiser, *J. Clin. Endocrinol. Metab.* **28**, 355 (1968); Y. S. Moon, B. K. Tsang, C. Simpson, D. T. Armstrong, *ibid.* **47**, 263 (1978); G. F. Erickson, A. J. W. Hsueh, M. E. Quigley, R. W. Rebar, S. S. C. Yen, *ibid.* **49**, 514 (1979); K. P. McNatty, A. Markis, C. DeGrazia, R. Osathanondh, K. J. Ryan, *ibid.* **51**, 1286 (1980).
11. J. S. Richards, in *Ovarian Follicular Development and Function*, A. R. Midgley and W. A. Sadler, Eds. (Raven, New York, 1979), p. 225.
12. G. S. Jones, S. Aksel, A. C. Wentz, *Obstet. Gynecol.* **44**, 26 (1974); R. L. Stonffer and G. D. Hodgen, *J. Clin. Endocrinol. Metab.* **51**, 669 (1980).
13. R. F. Casper and S. S. C. Yen, *Science* **205**, 408 (1979); A. Lemay, F. Labrie, A. Belanger, J.-P. Taynaud, *Fertil. Steril.* **32**, 646 (1979); K. L. Sheehan, R. F. Casper, S. S. C. Yen, *ibid.*, in press.
14. A. T. Hertig and J. Rock, *Am. J. Obstet. Gynecol.* **4**, 149 (1974); T. S. Kosasa, L. A. Levesque, D. P. Goldstein, M. L. Taymor, *J. Clin. Endocrinol. Metab.* **36**, 622 (1973); G. D. Braunstein, G. M. Grodin, J. Vaitukaitis, G. T. Ross, *Am. J. Obstet. Gynecol.* **115**, 447 (1973); K. J. Catt, M. L. Dufau, J. L. Vaitukaitis, *J. Clin. Endocrinol. Metab.* **40**, 537 (1975); D. R. Mishell, R. M. Nakamura, J. M. Barberia, F. H. Thorneycroft, *Am. J. Obstet. Gynecol.* **118**, 990 (1974).
15. We thank A. Lein for critical comments. Supported by NIH, NICHD contracts N01HD-92842, and HD-12303, and the Mellon, Rockefeller, and Clayton foundations. S.S.C.Y. is a senior investigator of the Clayton Foundation.
* Correspondence should be addressed to S.S.C.Y.

31 August 1981; revised 16 October 1981

Actin Distribution Patterns in the Mouse Neural Tube During Neurulation

Abstract. *With the use of antibodies to actin and indirect immunofluorescent techniques regions of increased actin concentration were demonstrated first in basal and later in apical areas of mouse neuroepithelial cells. These patterns of staining corresponded to shape changes observed in cranial neural folds as they initially elevated from the neural plate and later moved toward the midline.*

Microfilaments have long been thought to play a role in the process of neurulation. Ever since Baker and Schroeder (*1*) described the presence of apical microfilaments in amphibian embryos, these structures have been implicated as the driving force responsible for apical constriction of neuroepithelial cells (*1–4*). This apical constriction in turn leads to the creation of "flask-shaped" cells that aid in elevation of the neural folds resulting in the process of neurulation (*2*).

Evidence for the contractility of these microfilaments is derived from their morphological similarities to other such filaments known to be composed of nonmuscle actin (*5, 6*). Additional evidence that neuroepithelial microfilaments contain actin has been provided by demonstrating the typical arrowhead pattern when such filaments from chick neuroepithelial cells are reacted with heavy meromyosin (*7*). Although these data strongly suggest that neuroepithelial microfilaments contain actin and play a contractile role, further characterization of actin distribution patterns in neurulating tissues would serve to substantiate this hypothesis. We have studied the distribution of actin in cranial folds of mouse embryos at different stages of neurulation using antibodies to actin and indirect immunofluorescent methods. Mouse embryos were selected because cranial neural folds are larger and assume a more complex shape in mammals than in anurans or urodeles. Thus, actin distribution patterns may also be more complex in mammals.

Antibodies to actin were prepared by injecting rabbits with highly purified chicken gizzard actin (*8*). These antibodies are specific for actin according to the following criteria: (i) the gizzard actin was purified by sodium dodecyl sulfate (SDS)–polyacrylamide gel electrophoresis (SDS-PAGE); (ii) the antibody bound to homogeneous gizzard, skeletal muscle, and cardiac actin when these were tested in a solid-phase assay; (iii) the antibody showed the expected immunofluorescent patterns such as stress fibers in fibroblasts and typical I-band staining in muscle fibers; and (iv) the antibody bound only to actin on overlays of nitro-

0036-8075/82/0108-0172$01.00/0

cellulose transfers of SDS-PAGE extracts of skeletal muscle, smooth muscle, heart, and brain.

Mouse embryos were collected at different stages of neurulation and fixed in Carnoy's fixative, dehydrated, and embedded in paraffin. Sections were cut at 4 μm and stained by flooding the slides for 1 hour with a phosphate buffered saline solution (FAS, Difco) of the antibody (1 mg/ml). The slides were then rinsed in buffer and the sections were reacted with fluorescein conjugated goat antibody to rabbit immunoglobulin G (IgG) (Miles Laboratories). Control sections were reacted with fluorescein conjugated IgG from nonimmunized rabbits or fractions absorbed with columns of actin coupled to agarose. The control sections showed no fluorescence.

Only the cranial fold region was examined and compared in all embryos. The patterns of actin distribution during early stages of neurulation are shown in Fig. 1. No specific localization of actin was observed at the primitive streak stage of development, that is, prior to initiation of neural fold elevation. At the two-somite stage, neural folds were elevating from the neural plate and actin was localized along the basal aspect of neuroepithelial cells; only patchy staining was observed in apical cell regions. By the four- to five-somite stage, apical patterns of actin localization appeared and staining of basal cell regions was absent. Later, as opposing neural folds continued to elevate and approached the midline, apical fluorescence was maintained (Fig. 2). Also at this time intense fluorescence was present deep within the neural groove and in the ectoderm cells that overlie the neurectoderm and are responsible for initiating contact between the folds. Finally, after closure and reorganization of the neuroepithelium beneath the closure site, apical fluorescence persisted, but with less intensity.

These changing patterns of actin distribution suggest the following. First, areas of high actin concentration are not restricted to apical regions of neuroepithelial cells. Second, there appears to be a redistribution of actin within neuroepithelial cells from basal areas during early stages of neurulation, to cell apices at slightly later stages. Third, a basal localization of actin in conjunction with fold morphology implies a role for the contractile protein in establishing the biconvex fold appearance characteristic of early somite stages.

The distribution of actin fluorescence is consistent with the shape changes occurring in the neural folds. Thus, prior to initiation of fold elevation actin is not localized in specific regions. Fluorescence then increases in basal cell areas at the same time the folds are assuming a biconvex appearance (Fig. 1). This result would be expected if increased concentrations of actin participate in this shape change. Theoretically, contraction of actin filaments in basal cell areas would create an inverted flask–shaped cell that would lead to the observed curvature. Finally, at the four- to five-somite stage when neural folds begin to swing around to assume a biconcave structure, the actin is apparently redistributed to apical regions to create the classical flask-shaped cell responsible for approximating folds into the midline.

Increased fluorescence associated with basal and apical cell regions pre-

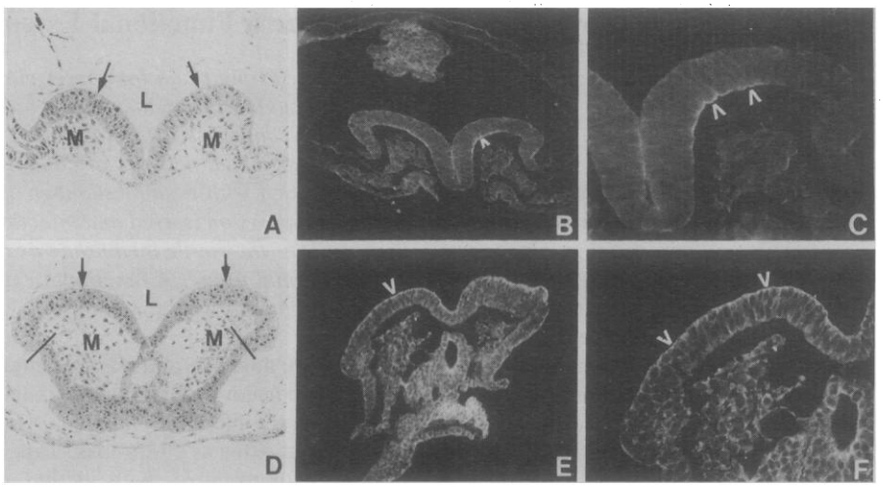

Fig. 1. Cross sections through the head folds of (A to C) a two-somite mouse embryo and (D to F) a five-somite mouse embryo. (A) The folds assume a biconvex shape with the neuroepithelium (arrows) continuous with the lateral plate ectoderm and the neural groove in the midline. (B and C) Micrographs showing actin distribution revealed by indirect immunofluorescent techniques. Although all the cells show some fluorescent activity because of the ubiquitous nature of actin, the heaviest staining is in the basal regions of neuroepithelial cells (arrowheads). (D) A clear line of demarcation has been established between neuroepithelium (arrows) and lateral plate ectoderm (bar), and the neural folds have assumed a flattened shape preparatory to continued elevation and closure. (E and F) Patterns of actin distribution revealed by indirect immunofluorescent techniques and demonstrating the apical concentration of the protein at this stage of development (arrowheads). *L*, prospective neural lumen; *M*, head fold mesenchyme. Magnifications: A, B, D, and E, ×110; C, ×275; F, ×215. (The sections were photographed with a Zeiss Universal microscope and Kodak Tri-X film.)

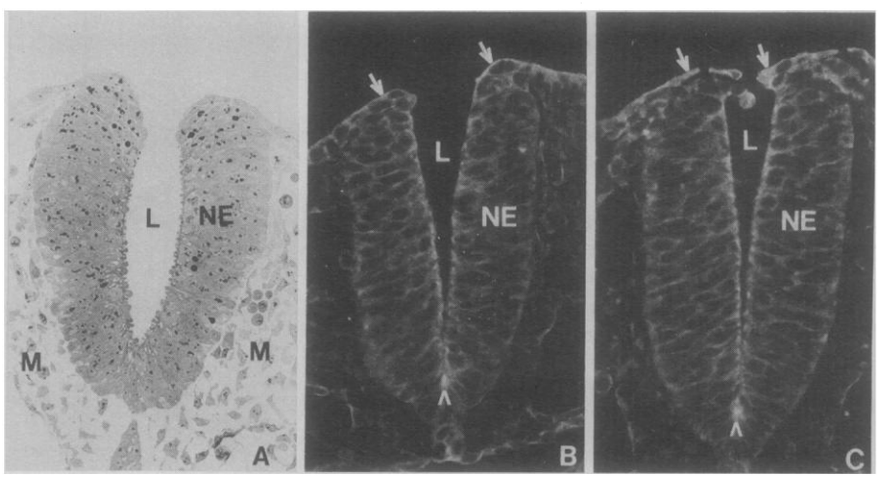

Fig. 2. (A to C) Cross sections through the prospective hindbrain of a neurulating mouse embryo. The neural folds have approached the midline and are about to make contact. Actin, as demonstrated by indirect immunofluorescent techniques, is localized in the apices of neuroepithelial cells (*NE*) and in the overlying ectoderm (arrows). In (C) these ectoderm cells are reaching for the opposite side and are about to make contact. Another focal concentration of fluorescent activity lies deep within the neural groove (arrowhead); *L*, prospective neural lumen; *M*, mesenchyme. Magnification: ×100.

sumably is due to an increase in the actin concentration in these areas. However, this pattern may also be related to an active constriction of putative microfilaments leading to a condensation of actin which is reflected as increased fluorescence. In either case it seems unlikely that the increased fluorescence is secondary to changes in morphology, since redistribution of intense staining precedes bending of the neural plate in these areas. Furthermore, ultrastructurally an increase in apical microfilaments during neurulation has been well documented (*1–4*) and increased fluorescence in this region is consistent with this observation.

Increased fluorescence in the neural groove of later-stage embryos suggests that this region may be a focal point for contractile activity, but may also represent overlap of apical cell areas that are close together in the groove. The intense fluorescence in overlying ectoderm cells suggests an active role for this tissue in the process of neurulation as proposed by Schroeder (*9*). This localization of fluorescence may also be related to the role these cells play in bridging the gap between folds and for making initial contact. This phenomenon is an active process, and ectoderm cells extend numerous filopodia to initiate contact between opposing sides. Perhaps contractile proteins play a role in this process as they do in fibroblast migration.

Thus we have shown that the pattern of actin distribution is consistent with the hypothesized role of this contractile protein during mouse neurulation. Our results provide new evidence that a redistribution or reorganization of actin in cranial neural folds occurs at the time that folds initiate the change from a biconvex morphology to a biconcave tube-like structure. This changing pattern appears to be related to the alterations in cranial neural fold morphology that are more complex in mammalian embryos than in avian or amphibian embryos. However, whether or not this changing pattern of fluorescence coincides with the presence of microfilaments remains to be determined.

T. W. SADLER
D. GREENBERG
P. COUGHLIN

Department of Anatomy, College of Medicine, University of Cincinnati, Cincinnati, Ohio 45267

J. L. LESSARD

Division of Cell Biology, Children's Hospital Research Foundation, Cincinnati 45229

References and Notes

1. R. C. Baker and T. E. Schroeder, *Dev. Biol.* **15**, 432 (1967).
2. T. E. Schroeder, *Int. J. Neurosci.* **2**, 183 (1971).
3. B. Burnside, *Am. Zool.* **13**, 989 (1973).
4. P. Karfunkel, *Int. Rev. Cytol.* **38**, 245 (1974).
5. R. D. Goldman, E. Lazarides, R. Pollack, K. Weber, *Exp. Cell Res.* **90**, 333 (1975).
6. T. D. Pollard, E. Sheldon, R. Weihing, E. Korn, *J. Mol. Biol.* **50**, 91 (1979).
7. R. G. Nagele and H. Y. Lee, *J. Exp. Zool.* **213**, 391 (1980).
8. J. L. Lessard, D. Carlton, D. C. Rein, R. Akeson, *Anal. Biochem.* **94**, 140 (1979).
9. T. E. Schroeder, *J. Embryol. Exp. Morphol.* **23**, 427 (1970).
10. This work was supported by NIH grants HD-14220 and HD-12295 and by the Muscular Dystrophy Association.

14 August 1981; revised 26 October 1981

Wound Tissue Can Utilize a Polymeric Template to Synthesize a Functional Extension of Skin

Abstract. *Prompt and long-term closure of full-thickness skin wounds in guinea pigs and humans is achieved by applying a bilayer polymeric membrane. The membrane comprises a top layer of a silicone elastomer and a bottom layer of a porous cross-linked network of collagen and glycosaminoglycan. The bottom layer can be seeded with a small number of autologous basal cells before grafting. No immunosuppression is used and infection, exudation, and rejection are absent. Host tissue utilizes the sterile membrane as a culture medium to synthesize neoepidermal and neodermal tissue. A functional extension of skin over the entire wound area is formed in about 4 weeks.*

Excessive fluid loss and massive infection are two major problems immediately threatening the life of an individual who has suffered extensive skin loss. This is the case, for example, with victims of deep burns extending over more than 50 percent of the body. Current treatment emphasizes fluid resuscitation and prompt closure of wounds with autografts, cadaver skin, or pig skin following the excision of dead tissue (*1*). Failure to achieve closure of burn wounds within 3 to 7 days after injury significantly increases the probability that the patient will die (*1*).

We have developed a bilayer polymeric membrane that promptly and aseptically closes skin wounds in animals and humans while serving as a template for the construction of a functional extension of the skin. Our design has evolved over the past 11 years from studies of guinea pigs (*2*). The top layer of the membrane is a silicone elastomer and the bottom layer is a highly porous, covalently cross-linked network of bovine hide collagen and glycosaminoglycan (GAG) (Fig. 1) (*3*). We have achieved reproducible conditions under which autologous basal cells, seeded into the

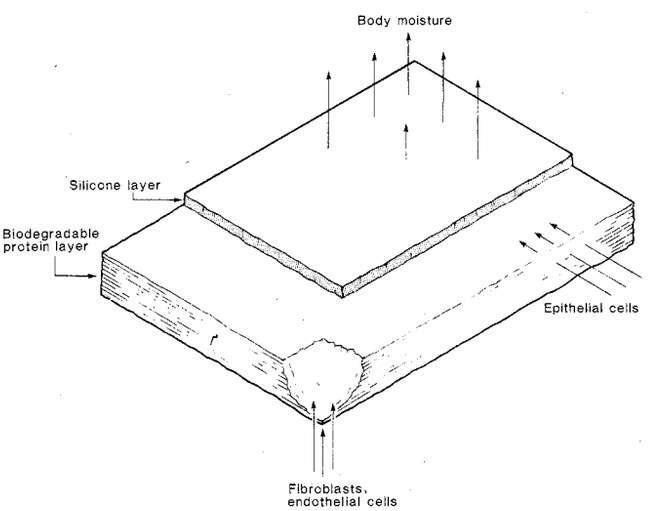

Fig. 1. Schematic representation of a standard version of the noncellular bilayer polymeric membrane (stage 1). The moisture flux through the layers ranges from 1 to 10 mg/cm^2 per hour. Fibroblasts and endothelial cells migrate into the bottom layer while epithelial cell sheets advance from the wound edge in the plane of the membrane, between the two layers. The top layer is a conventional medical-grade silicone which undergoes cross-linking at room temperature following exposure to ambient moisture. The bottom layer is a cross-linked network of collagen and chondroitin 6-sulfate, a GAG (bound GAG content 8.2 ± 0.8 percent by weight, average molecular weight between cross-links 12,750 ± 3,300, pore volume fraction 96 ± 2 percent, mean pore size 50 ± 20 μm). The collagen-GAG layer undergoes biodegradation at a controlled rate and is replaced by neodermal tissue while the silicone layer is spontaneously ejected following formation of a confluent neoepidermal layer under it. Stage 2 membranes are identical except that autologous epidermal (basal) cells are seeded into the membranes before grafting.

0036-8075/82/0108-0174$01.00/0